Mini-SAR: an imaging radar experiment for the Chandrayaan-1 mission to the Moon

Paul Spudis[1,*], Stewart Nozette[1], Ben Bussey[2], Keith Raney[2], Helene Winters[2], Christopher L. Lichtenberg[3], William Marinelli[4], Jason C. Crusan[4] and Michele M. Gates[4]

[1]Lunar and Planetary Institute, 3600 Bay Area Blvd, Houston, TX 77058, USA
[2]Applied Physics Laboratory, Laurel MD 20723, USA
[3]Naval Air Warfare Center, China Lake, CA 93555, USA
[4]National Aeronautics and Space Administration, Washington, DC 20546, USA

Mini-SAR is a single frequency (S-band; 13-cm wavelength) Synthetic Aperture Radar (SAR) in a lightweight (~9 kg) package. Previous Earth- and space-based radar observations of the permanently shadowed regions of the lunar poles have measured areas of high circular polarization ratio consistent with volume scattering from water ice buried at shallow (0.1–1 m) depths. This detection is not definitive because of poor viewing geometry and a limited number of observations. Mini-SAR utilizes a unique hybrid polarization architecture, which allows determination of the Stokes parameters of the reflected signal, intended to distinguish volume scattering (caused by the presence of ice) from other scattering mechanisms (e.g. sub-wavelength scale surface roughness).

Keywords: Ice, Moon, poles, radar, SAR.

Introduction

THE nature and distribution of deposits in the permanently shadowed polar terrain of the Moon[1] has been the subject of considerable controversy. Initially, Arecibo monostatic radar measured the circular polarization ratio (CPR) in the region of the lunar south pole; these data were interpreted to indicate the possible presence of ice on the lower wall of Shackleton crater[2]. Data collected by the Clementine bistatic radar experiment[3–5] also revealed anomalous CPR in Shackleton as a function of bistatic angle, suggesting the presence of patchy, 'dirty', ice deposits on the lower Earth-facing wall. The high CPR region observed deepest within Shackleton crater also has a local angle of incidence of 50° (estimated by Stacy[2]). This region has a monostatic CPR of 1.19 ± 0.12, comparable to the radar bright feature at the north pole of Mercury measured by Harmon and Slade[6]. Stacy[2] noted that because this area may be permanently shadowed, the coherent backscatter opposition effect (CBOE) from ice deposits might be responsible for its elevated CPR.

Subsequently, higher resolution Arecibo data were reported to be inconsistent with this claim[7,8], and it was suggested that all anomalous high CPR areas observed by Arecibo, near the lunar south pole, were caused by rough surfaces (Figure 1) as only some portion of these areas was believed to be permanently shadowed. It was also postulated[9] that the Clementine polarization anomaly is due to roughness and/or random noise in the data and not by the presence of ice. Campbell *et al.*[7] suggested that the high CPR areas within Shackleton could be due to diffuse backscatter from wavelength scale structures since other non-shadowed structures exhibit similar behaviour.

If the enhanced backscatter in Shackleton has a contribution from ice, there could be differences in scattering behaviour between areas in permanent sunlight and areas in permanent shadow. Examination of similar craters from illuminated regions of the Moon (e.g. Shumberger G) showed different radar scattering characteristics[7]. The upper part of the radar facing inner rims of illuminated craters has greater backscatter cross-sections, which appear to be associated with geological structures; the high CPR in Shackleton is deeper, isolated, discontinuous, and not associated with other geological units, but the crater bottom is not observable from Earth[10]. Additionally, a high degree of correlation exists between the decreasing epithermal neutron flux and the shadowed terrain at the lunar south pole, including Shackleton which has been attributed to water ice deposits[11–13].

The lunar ice controversy cannot be resolved with existing data. New measurements are required and mapping these deposits from lunar orbit is essential to fully characterize them. Previous studies of mechanisms of deposition and preservation of lunar polar ice suggest that it may be buried at a depth of 0.1–2 m (ref. 13). An imaging radar that could probe the regolith at depth for ice and meet the stringent mass and power constraints of the Chandrayaan-1 spacecraft was not spaceflight proven. Previously flown NASA scientific radars displayed the opposite trend, getting larger and requiring more power.

*For correspondence. (e-mail: spudis@lpi.usra.edu)

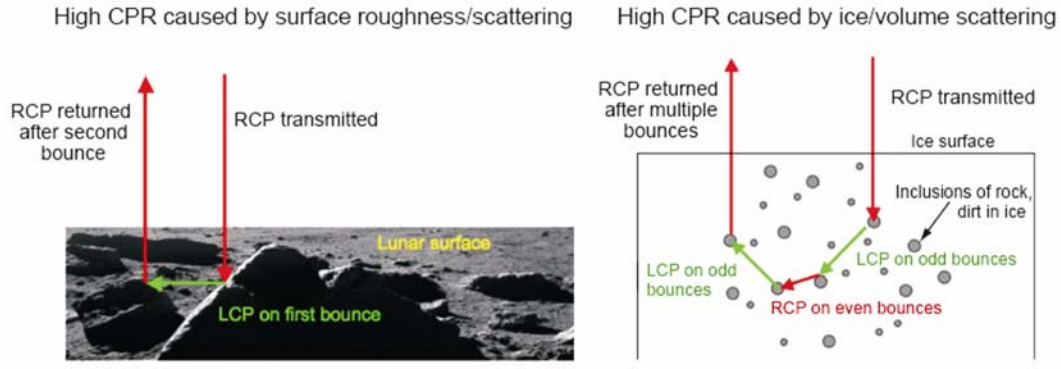

Figure 1. Elevated circular polarization ratio caused by ice (volume) or roughness (surface) scattering (from Spudis[10]).

Table 1. Mini-SAR parameters

	SAR	Scatterometer
System parameters		
Altitude	100 km	
Frequency	2.38 GHz	
Spacecraft velocity	1631 m/s	
Range swath	8 km	N/A
Strip length	325 km	300 km
Antenna parameters		
Antenna length	1.37 m	
Antenna width	0.925 m	
Boresight gain	26.1 dB	
Antenna efficiency	53%	
Grazing angle	55 deg	90 deg
Image quality parameters		
Noise equivalent sigma naught	–30 dB	–15 dB
Slant range resolution	86 m	N/A
Ground range resolution	150 m	N/A
Azimuth resolution	150 m	1000 m
Multiplicative noise ratio	–12 dB	
RF parameters		
Transmit pulse width	84 μs	83 μs
Chirp bandwidth	2.1 MHz	
Peak power at transmitter port	40 W	
Average transmitted power	11 W	
Losses between transmitter and antenna	1.63 dB	
System noise temperature	620 K	
Digital parameters		
PRF	3100 Hz	3750 Hz
No samples/pulse	1119	1186
A/D sampling frequency	8.2 MHz	
Number of A/D bits per sample	8	
Number of receive channels	2	
Peak data rate into SSDR	187.43 Mbps	
Average data rate into SSDR during collect	6.22 Mbps	5.24 Mbps
Collect time/orbit	6 min	

Over the previous decade, the Department of Defense (DoD) and commercial industry had made significant strides in developing advanced lightweight RF technology. The unique constraints of a lunar mission (close range, limited duty cycle over the poles) and the transition of advanced lightweight RF technology afforded a solution which met the payload constraints of both the Chandrayaan-1 and LRO spacecraft.

Description of investigation

The Mini-SAR experiment is designed to gather data on the scattering properties of terrain in the polar regions of the Moon. The specific instrument requirements and data collection modes are shown in Tables 1 and 2. In brief, the Mini-SAR is a single-frequency, hybrid polarity (Figure 2) imaging radar designed to collect information about the scattering properties of the permanently dark areas near the lunar poles at optimum viewing geometry. Additionally, Mini-SAR will map the terrain of these areas, invisible to normal imaging sensors.

The Chandrayaan-1 Mini-SAR will map both regions of the lunar poles systematically with a resolution of 75 m/pixel. The Chandrayaan-1 instrument utilizes a hybrid polarity architecture (Figure 2) and will collect data of sufficient quality to identify areas of unusual scattering properties. Under the proposed observational constraints, we can identify areas of high CPR which could be caused by ice deposits. When supported by other remote sensing data (e.g. neutron spectroscopy, shadow and lighting, thermal environment), the Mini-SAR measurements should provide more conclusive evidence as to the likelihood that ice deposits occur in permanently shadowed areas.

The Mini-SAR antenna architecture is shown in Figure 2. This architecture is unique in planetary radar; it transmits right circular radiation and receives the horizontal (H) and vertical (V) polarization components coherently, which are then reconstructed as Stokes' parameters during the data processing. This approach saves weight by eliminating a set of circulator elements, improving efficiency; by providing H and V signals directly to the processor, the polarization properties of the backscattered field may be fully characterized as Stokes' parameters, as shown in Figure 3. The Stokes' parameters may be used

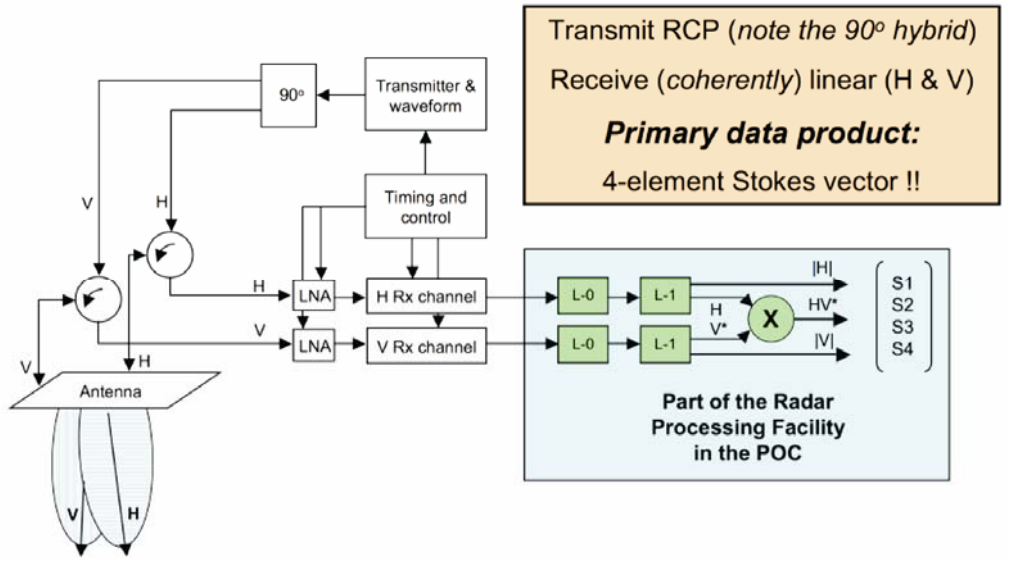

Figure 2. Block diagram of Mini-SAR, showing the hybrid polarity architecture used to gather information on lunar surface Stokes parameters.

Table 2. Mini-SAR instrument characteristics

Antenna	
Size	60 cm × 180 cm × 5 cm
Mass	3.3 kg
Electronics	
Size	17 cm × 17 cm × 10 cm
Mass	3.1 kg
Connections, mounting hardware, cabling mass	1.8 kg

to describe the full range of polarization properties of the surface which should aid in distinguishing polarization effects caused by volumetric scattering (ice) and those caused primarily by surface textural properties (e.g. wavelength scale roughness, double bounce reflections; Figure 1).

Mini-SAR probes the lunar regolith at S-band (13 cm) frequency, providing additional information on the physical properties of the upper meter or two of lunar surface. Stokes' parameter-based products (e.g. CPR, degree-of-depolarization, degree-of-linear polarization, phase 'double bounce') have a number of significant advantages over traditional radar systems: less hardware is needed, resulting in fewer losses and a 'cleaner', simpler flight instrument. The signal levels are comparable (within ~2 dB) in both channels, allowing relatively relaxed specifications on channel-to-channel cross talk and more robust phase and amplitude calibration. The processor has a direct view through the entire receiver chain, including the antenna receive patterns (e.g. gain and phase; Figure 2). The design allows selective Doppler weighting to maximize channel–channel coherence (e.g. reduce the H&V beam mismatch). As CPR is less sensitive to channel imbalance by at least a factor of 2 with respect to explicit RCP/LCP, Stokes parameter-based backscatter decomposition strategies can help distinguish 'false' from 'true' high CPR areas (e.g. analysis of '$m - \delta$' feature space; see Raney[14]).

Our concept of operations is shown in Figure 4. Because it is a high data rate instrument, Mini-SAR has been allocated periods of observation time during the intervals when visual imaging is curtailed by lunar surface illumination conditions (Figure 4). Four such periods occur during the nominal two-year surface mapping Mission of Chandrayaan-1; each is of 30 days duration and Mini-SAR requires 28 days to obtain complete coverage of the lunar poles. We plan to map both poles during a single period (Figure 5); over the course of the nominal mission, we will obtain complete coverage of both poles in both left-looking and right-looking geometries, which will help eliminate reflection ambiguities. Each mapping coverage includes SAR images of the surface in terms of the four Stokes parameters, which will be combined into maps of various properties, including CPR and other derived parameters that can help us to distinguish surface from volume scattering. In addition to normal SAR mapping, Mini-SAR can collect radar scatterometry via a 33° roll of the spacecraft such that its antenna points straight down (Figure 5). Because even in a perfectly polar orbit, the groundtrack will 'wobble' around the pole 1.5° due to the inclination of the lunar spin axis, it is possible to slightly roll the spacecraft to SAR image the pole at higher incidence angles (Figure 6). If possible, we will implement this strategy on a non-impact basis to the mission in order to 'fill-in' the SAR coverage gap around both poles.

Additional observations of polar deposits of interest may be possible during the mission of the Lunar Recon-

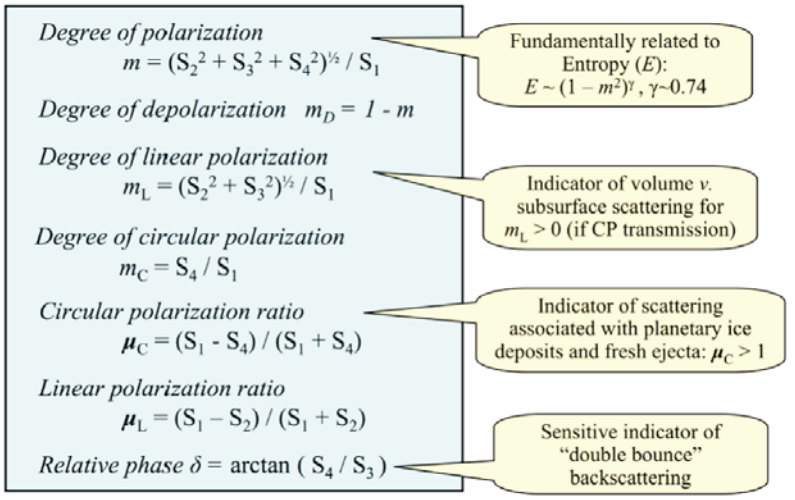

Figure 3. Derived 'daughter' Stokes parameters and what they mean.

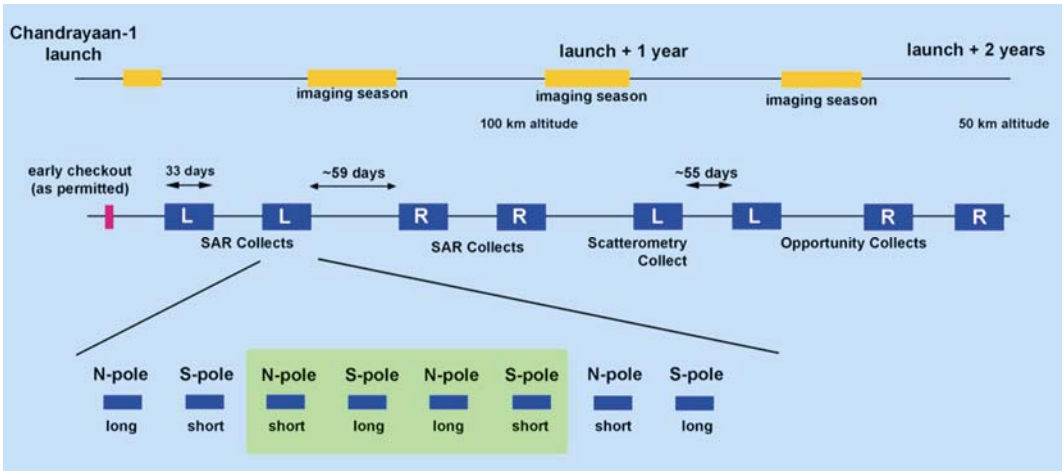

Figure 4. Chandrayaan-1 Mini-SAR measurement timeline.

naissance Orbiter. By the end of the nominal LRO mission, we will have regional S-band SAR maps from Mini-SAR on Chandrayaan-1, 20 targeted SAR strips from Mini-RF on LRO, and correlation with higher resolution neutron and other data from LRO. Mini-SAR could use observation opportunities from an extended LRO mission to acquire more data of both polar and non-polar regions. These are currently defined as supplemental science goals, including additional SAR and interferometry data and bistatic options with the Chandrayaan-1 instrument. Because both Chandrayaan-1 and LRO will be in lunar orbit at the same time, the Chandrayaan-1 Mini-SAR and LRO Mini-RF units were designed to operate cooperatively in a bistatic mode, with Chandrayaan-1 transmitting and LRO receiving in S-band radar data. Both orbits cross at the poles and it may be possible to obtain bistatic measurements of selected high CPR targets to determine if high CPR is correlated with the bistatic (phase) angle. Such a measurement would be most deterministic of volume scattering caused by ice deposits and may be obtained during the LRO extended mission.

Instrument description

The Mini-SAR system consists of an electronics box and antenna (Figure 7); data handing and storage are handled by the Chandrayaan-1 spacecraft data subsystem. The Mini-SAR electronics box contains the waveform generator, digital circuits, receiver and transmitter (Figure 2). The electronics box is mounted on the back of the moon-facing panel on the Chandrayaan-1 spacecraft. System specifications are shown in Table 1.

A form-core, cross linears array antenna (Figure 7) allows a broadband approach with a single antenna panel, without any deployable mechanisms (e.g. feeds) while meet-

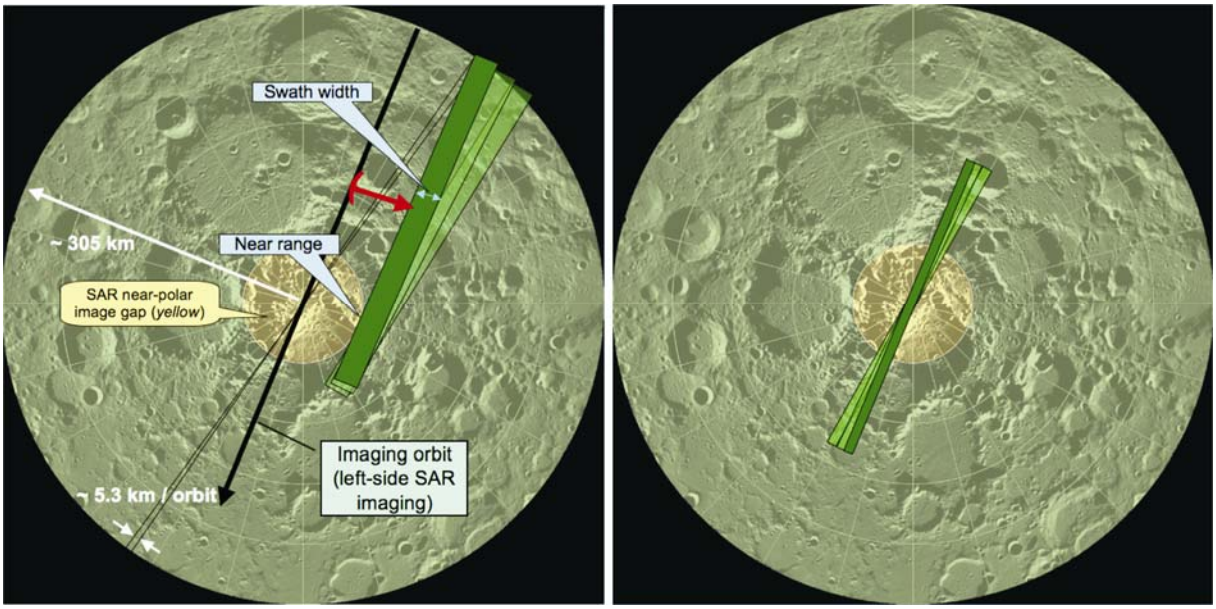

Figure 5. Nominal SAR and scatterometry polar mapping strategy.

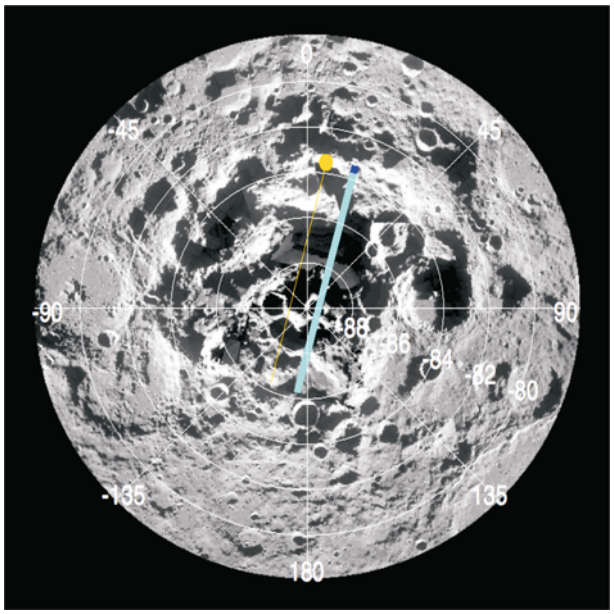

Figure 6. High-incidence SAR mapping of Shackleton crater interior.

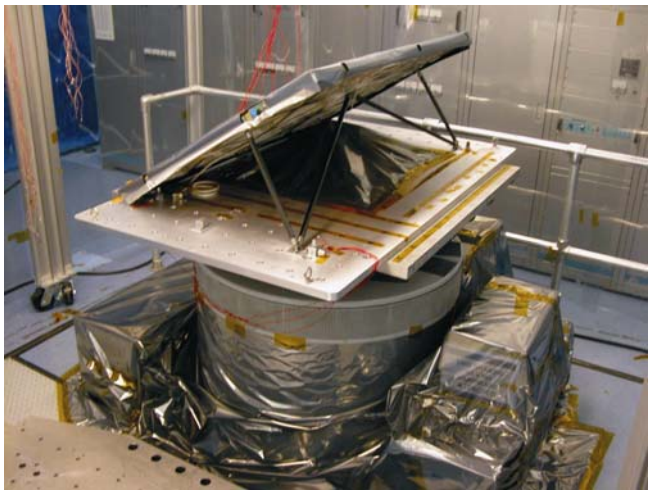

Figure 7. Mini-SAR antenna during testing.

ing stringent weight and volume constraints. The thermal design, materials selection, manufacturing, and test qualification heritage of Chandrayaan-1 Mini-SAR antenna were applied also to the LRO Mini-RF unit. The combined mass of the antenna and electronics is less than 9 kg (Table 2).

A processor module based on a heritage OBC 695 and associated firmware and software, developed by Surrey Satellite Technology Ltd (SSTL) controls the Mini-SAR system. Data handling and processing is done via the Chandrayaan-1 spacecraft solid state memory and data handling systems.

Instrument calibration

Laboratory calibration data was acquired before launch during spacecraft integration and test. The overarching goal of these activities was to ensure production of a calibrated instrument. All waveforms in the waveform table were tested on brass board hardware while selected waveforms were tested on flight hardware. Additional waveform testing was done on the flight instrument during thermal vacuum temperature ramp cycles. Internal calibration data are acquired every time Mini-SAR takes a science data collect; a chirp, noise, and tone calibration is done both immediately before, and immediately after a data collect.

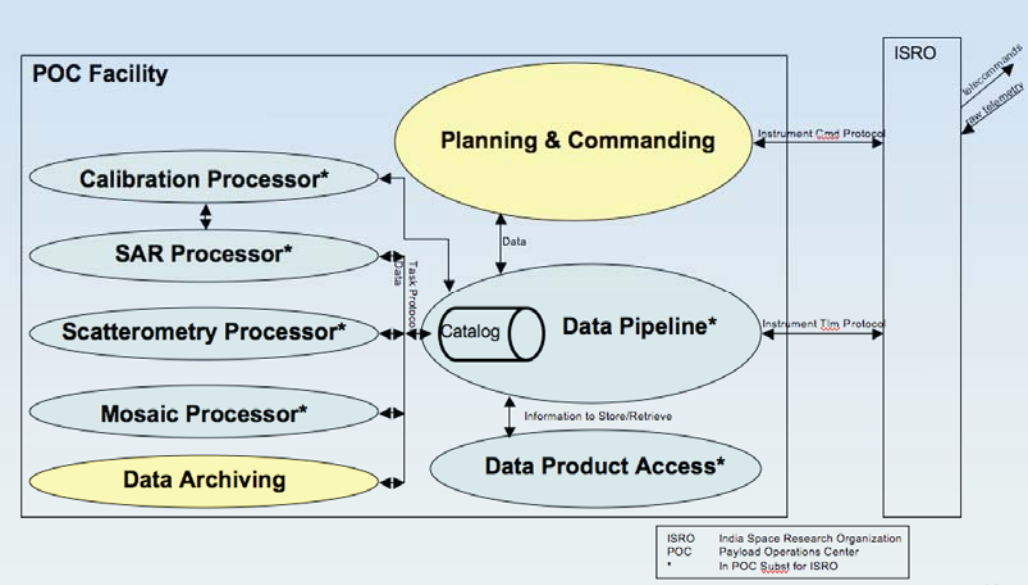

Figure 8. Payload Operations Center overview of block diagram.

External calibration is planned en route to the Moon by taking data using ground-based assets. During the translunar cruise we will conduct calibration measurements with the Greenbank Radio Telescope in West Virginia, USA. A transmitted signal from Mini-SAR is received by Greenbank while the antenna boresight is scanned via spacecraft attitude changes over a range of angles. We will scan the antenna, parallel to the Chandrayaan-1's orbit plane (which is 20° off the equatorial plane) while compensating for Earth rotation, at 0.4° per second 12° in one direction, then back to boresight, then 12° in the other direction, then back to boresight. Whilst scanning, Mini-RF will transmit for 40 ms every 1.25 s, corresponding to an angle change between transmits of 0.5°. The scan should take approximately two minutes to complete. After the spacecraft is rolled 90° (four minutes), the scan is repeated for the next plane for about 2 min. Next repeat the scan for the new plane, which will take another two minutes. The total time for the calibration should be approximately eight minutes.

During commissioning after lunar orbit insertion, Mini-SAR can acquire calibration data before the nominal science mapping begins. At least two lunar equatorial areas will be imaged; these data takes will observe a region of the Moon of well-known geological and scattering properties (maria and highlands) at viewing geometries identical to the data to be acquired for the polar regions. These calibration takes cover latitudes from 10° to –10° at 33° west longitude and 33° east longitude. Since each of these data takes would require approximately six minutes and LRO Mini-SAR may only transmit for four minutes, each equatorial target will be sub-divided into two separate data acquisitions. Mini-SAR would image from 10°N to 2°S at 33° longitude on one orbit and then on the next orbit from 2°N to 10°S. The longitude of this second data take would be either 32° or 34°. Every six months there will be a window, centred around the dawn-dusk orbit, where calibration activities can be conducted, particularly calibration activities that require a spacecraft maneuver. During these times, Mini-SAR can conduct the following calibration activities, in priority order; transmit calibration to Greenbank using the cislunar transit procedures, two, 1-minute duration nadir mode observations (ideally in a polar region), and a receive calibration from the Arecibo radiotelescope using the same scan pattern used for the transmit calibrations.

Data analysis and interpretation

A joint Chandrayaan-1/LRO Payload Operations Center (POC) has been constructed at APL to support both the Mini-SAR and Mini-RF experiments. The POC will provide the following functions: forward Science Team command sequences to ISRO/GSFC (Goddard Space Flight Center, Maryland, USA) receive raw telemetry from ISRO/GSFC, process raw telemetry, produce SAR images and mosaics, catalog the data for the ISRO and NASA Planetary Data Systems (PDS) and other data repositories. The POC architecture and data flow are shown in Figure 8.

After the raw radar data are processed into digital mosaics of SAR imagery and Stokes parameters, we will compare these data to other lunar data, specifically topographic maps and images showing the likely locations of permanently dark areas, including temperature information on possible cold traps. The search will focus on areas of high CPR that occur exclusively in these cold traps;

any ice present on the Moon must be located in these areas. Study of the scattering properties of these zones will be greatly enhanced by comparison with other data sets, including neutron flux maps and gamma-ray information on the distribution of surface hydrogen.

The Mini-SAR experiment will both map a previously unknown region of the Moon and collect information relevant to the possible existence of water/ice on the Moon. Such deposits are important for both scientific and operational reasons; from a scientific perspective, ice deposits would be evidence of previously unappreciated lunar processes and history. From an operational viewpoint, ice on the Moon is a concentrated and easily convertible form of hydrogen and oxygen, available to enable the Moon's habitation and use by humans as they move off-planet into the Solar System.

1. Arnold, J. R., Ice in the lunar polar regions. *J. Geophys. Res.*, 1979, **84**, 5659–5668.
2. Stacy, N. J. S., High-resolution synthetic aperture radar observations of the moon, Ph D dissertation, Cornell University, Ithaca, NY, 1993.
3. Nozette, S. *et al.*, The Clementine bistatic radar experiment. *Science*, 1996, **274**, 1495–1498.
4. Nozette, S., Shoemaker, E. M., Spudis, P. D. and Lichtenberg, C. L., The possibility of ice on the Moon. *Science*, 1997, **278**, 144–145.
5. Nozette, S., Spudis, P. D., Robinson, M., Bussey, D. B. J., Lichtenberg, C. and Bonner, R., Integration of lunar polar remote-sensing data sets: Evidence for ice at the lunar south pole. *J. Geophys. Res.*, 2001, **106**, 23253–23266.
6. Harmon, J. K. and Slade, M. A., Radar mapping of Mercury: Full-disk Doppler delay images. *Science*, 1992, **258**, 640–643.
7. Campbell, D. B., Campbell, B. A., Carter, L. M., Margot, J.-L. and Stacy, N. J. S., No evidence for thick deposits of ice at the lunar south pole. *Nature*, 2006, **443**, 835–837.
8. Stacy, N. J. S., Campbell, D. B. and Ford, P. G., Arecibo Radar Mapping of the Lunar Poles: A Search for Ice Deposits. *Science*, 1997, **276**, 1527–1530.
9. Simpson, R. A. and Tyler, G. L., Reanalysis of Clementine bistatic radar data for the lunar south pole. *J. Geophys Res.*, 1999, **104**, 3845–3862.
10. Spudis, P. D., Ice on the Moon. *The Space Review*, 2006; http://www.thespacereview.com/article/740/1
11. Elphic, R. C., Eke, V. R., Teodoro, L., Lawrence, D. J. and Bussey, D. B. J., Models of the distribution and abundance of hydrogen at the lunar south pole. *Geophys. Res. Lett.*, 2007, **34**, L13204, doi:10.1029/2007GL029954.
12. Feldman, W. C., Maurice, S., Binder, A. B., Barraclough, B. L., Elphic, R. C. and Lawrence, D. J., Fluxes of fast and epithermal neutrons from lunar prospector: Evidence for water Ice at the lunar poles. *Science*, 1998, **281**, 1496–1500.
13. Feldman, W. C., Lawrence, D. J., Elphic, R. C., Barraclough, B. L., Maurice, S., Genetay, I. and Binder, A. B., Polar hydrogen deposits on the Moon. *J. Geophys. Res.*, 2000, **105**, 4175–4195.
14. Raney, R. K., Hybrid-polarity SAR architecture. *IEEE Trans. Geosci. Remote Sensing*, 2007, **45**, 3397–3404.

ACKNOWLEDGEMENTS. We thank NASA's Spaceflight Operations Mission Directorate and the Exploration Systems Mission Directorate, and the Department of Defense for supporting the Mini-SAR project. This paper is Lunar and Planetary Institute Contribution Number 1444.